

P2Y₁₂R Blockade Attenuates LPS-Induced Acute Lung Injury Associated with Suppression of Inflammasome-Mediated Pyroptotic Signaling

Lian-Fang Zhang¹, Xiao-Ming Lin¹, Zi-Heng Zeng², Rong-Cheng Xie¹, Li-Tao Yi², Jie-Fei Ma^{1,3}

¹Department of Critical Care Medicine, Zhongshan Hospital (Xiamen), Fudan University, Xiamen, Fujian, 361015, People's Republic of China;

²Department of Chemical and Pharmaceutical Engineering, College of Chemical Engineering, Huaqiao University, Xiamen, Fujian, 361021, People's Republic of China; ³Department of Critical Care Medicine, Zhongshan Hospital, Fudan University, Shanghai, 200032, People's Republic of China

Correspondence: Jie-Fei Ma, Department of Critical Care Medicine, Zhongshan Hospital (Xiamen), Fudan University, 668 Jinhu Road, Xiamen, Fujian, 361015, People's Republic of China. Email majiefei@zs-hospital.sh.cn; Li-Tao Yi, Department of Chemical and Pharmaceutical Engineering, College of Chemical Engineering, Huaqiao University, 668 Jimei Avenue, Xiamen, Fujian, 361021, People's Republic of China, Email litaoyi@hqu.edu.cn

Purpose: Acute lung injury (ALI) is characterized by excessive inflammation and cell death, with no specific pharmacological treatment. P2Y₁₂ receptor (P2Y₁₂R) is implicated in regulating inflammation, but their role in ALI remains unclear. This study investigates the effects of P2Y₁₂R antagonists including Clopidogrel, Prasugrel, and Ticagrelor on LPS-induced ALI in mice, focusing on inflammation and pyroptosis.

Methods: Mice were pre-treated with P2Y₁₂R antagonists before LPS administration. Lung injury was assessed via histology, wet/dry ratio, myeloperoxidase (MPO) activity, and inflammatory cytokine levels in bronchoalveolar lavage fluid (BALF). Gene and protein levels of IL-1 β , IL-6, TNF- α , and inflammasome components (NLRP3, ASC, Caspase-1, GSDMD) were measured. Ultrastructural changes were analyzed by transmission electron microscopy (TEM).

Results: P2Y₁₂R antagonists reduced histological injury, pulmonary edema, and inflammatory cytokines in BALF, with Ticagrelor showing the most prominent effects. Gene and protein levels of IL-1 β , IL-6, and TNF- α were decreased. P2Y₁₂R antagonists also inhibited inflammasome activation and pyroptosis. TEM analysis showed reduced organelle damage in treated groups.

Conclusion: P2Y₁₂R antagonists, particularly Ticagrelor, attenuate lung injury and were associated with suppression of the NLRP3/caspase-1/GSDMD pyroptotic signaling axis.

Keywords: P2Y₁₂ receptor, P2Y₁₂R, acute lung injury, ALI, NLRP3, pyroptosis

Introduction

Acute lung injury (ALI) and its more severe clinical manifestation, acute respiratory distress syndrome (ARDS), represent life-threatening pulmonary conditions that continue to challenge critical care medicine.¹ These syndromes develop through a complex interplay of pathological mechanisms, including diffuse alveolar epithelial and endothelial damage, robust inflammatory cell infiltration, dramatically increased microvascular permeability, and consequent protein-rich pulmonary edema. The clinical symptom is characterized by severe hypoxemia, bilateral pulmonary infiltrates, and significantly reduced lung compliance.² Despite decades of research and notable improvements in supportive care modalities such as lung-protective ventilation and fluid management strategies, mortality rates remain unacceptably high, hovering around 30–40% for moderate to severe cases.^{3,4} This persistent clinical challenge requires the critical need to develop effective pharmacological interventions that can modify the disease course rather than merely support organ function.

Recent advances have shed new light on ALI pathophysiology. Pyroptosis, a highly inflammatory form of regulated cell death mediated by gasdermin D (GSDMD) pore formation, has emerged as a critical contributor to lung injury progression.^{5,6} Importantly, preclinical studies have demonstrated that pharmacological inhibition of NLRP3 inflammasome assembly can attenuate lung injury severity, suggesting that targeting NLRP3 related pyroptosis may be a new strategy for ALI intervention.^{7,8}

The P2Y₁₂ receptor (P2Y₁₂R), a Gi-coupled purinergic receptor, has traditionally been viewed primarily through the lens of cardiovascular medicine due to its crucial role in platelet activation and arterial thrombosis.⁹ This perspective led to the development of P2Y₁₂R antagonists like clopidogrel, prasugrel, and ticagrelor as mainstays of antiplatelet therapy for acute coronary syndromes.¹⁰ However, a growing number of evidence from immunological studies has revealed that P2Y₁₂R is expressed not only on platelets but also on various immune cells (including macrophages and neutrophils) and vascular endothelial cells.^{11–13} These findings suggest that P2Y₁₂R signaling may participate in inflammatory regulation through mechanisms distinct from its thrombotic functions. However, there is no evidence showing the effects of P2Y₁₂R blockade on ALI until now.

Several standard methods are commonly employed to confirm pyroptosis in experimental settings.^{14,15} These include ultrastructural examination of cell swelling and membrane rupture by transmission electron microscopy, detection of inflammasome-related proteins such as NLRP3, cleaved caspase-1, and cleaved GSDMD, and quantification of pyroptotic cytokines IL-1 β and IL-18. In addition, functional cell death assays such as flow cytometry with Annexin V/propidium iodide staining or caspase-1 activity probes provide direct evidence of pyroptotic membrane rupture. Together, these complementary techniques form the basis of mechanistic studies of pyroptosis. Building on this framework, the present study investigated whether pharmacological P2Y₁₂R blockade could exert protective effects in experimental ALI beyond its established antiplatelet actions. Using a well-characterized murine model of lipopolysaccharide (LPS)-induced lung injury, we systematically evaluated three clinically available P2Y₁₂R antagonists including ticagrelor, prasugrel, and clopidogrel. Our central hypothesis posited that these agents would attenuate lung inflammation and tissue damage by interfering with the NF- κ B/NLRP3/GSDMD signaling axis, thereby reducing pyroptotic cell death and its inflammatory consequences.

Materials and Methods

Animals

8-week-old male C57BL/6 mice, 18–22 g, Specific Pathogen Free (SPF) grade, were purchased from Shanghai SLAC Laboratory Animals Center (Shanghai, China). The mice were fed pure water and sterile mouse pellets. The temperature was 23 \pm 2°C and the humidity was 40–70% day and night. All experimental protocols involving animals were approved by the Institutional Animal Ethics and Use Committee of Huaqiao University (A2024075). All experimental protocols were conducted in full compliance with the Regulation on the Administration of Laboratory Animals, 1988, and the Laboratory Animal-Guideline for Ethical Review of Animal Welfare, 2018 of People's Republic of China.

Chemicals and Reagents

P2Y₁₂R antagonists including Ticagrelor (M3069), Prasugrel (M2234), and Clopidogrel (M3280) were purchased from Abmole (Houston, USA). BCA protein assay kit (P0012) was purchased from Beyotime (Shanghai, China). MPO kit (BC5715) was purchased from Solarbio (Beijing, China). RayPlex Mouse Inflammation Array kit (FAM-INF-1-96) was purchased from RayBiotech (Peachtree Corners, USA). TLR4 (PA5-142481, for Immunofluorescence), P2Y₁₂R (702516), NLRP3 (MA5-32255, for Immunofluorescence), NLRP3 (PA5-79740, for Western blot), ASC (PA5-50915), Caspase-1 (MA5-32137, for Immunofluorescence), GSDMD (PA5-116815, for Immunofluorescence), GSDMD (MA5-44666, for Western blot), IL-1 β (710331), and IL-18 (PA5-79481) were purchased from ThermoFisher (Waltham, USA). pNF- κ B (ab32536) were purchased from Abcam (Cambridge, USA). TLR4 antibody (GB11519, for Western blot) was purchased from Servicebio (Wuhan, China). Cleaved Caspase-1 antibody (89332, for Western blot) was purchased from Cell Signaling Technology (Danvers, USA). β -actin antibody (HRP-66009) and CoraLite[®] Plus 488-Annexin V and PI Apoptosis Kit (PF00005) were purchased from Proteintech (Wuhan, China).

ALI Establishment and Drug Administration

C57BL/6 male mice were randomly divided into the following 5 groups: control group (Control), LPS-induced ALI group (ALI), LPS+Clopidogrel group (Clopidogrel, 25 mg/kg), LPS+Prasugrel group (Prasugrel, 2 mg/kg), LPS+Ticagrelor group (Ticagrelor, 40 mg/kg), 8 animals in each group. Clopidogrel, Prasugrel, and Ticagrelor were pre-administered for 7

consecutive days. Control and LPS groups were administered with equal amount of sterile saline for 7 consecutive days. One hour after the last dose, animals in the LPS groups were injected intraperitoneally with LPS (5 mg/kg). The doses of Ticagrelor, Prasugrel, Clopidogrel, and LPS were selected based on the previous studies.^{16–19}

To obtain the quantitative data for pyroptotic cell, a dependent experiment was conducted, 3 animals in each group. The groups were set as the same described above.

Preparation of Bronchoalveolar Lavage Fluid (BALF)

Following experimental interventions, BALF was obtained from euthanized mice through tracheal cannulation of the left lung. After centrifugation (800 × g, 15 min), protein concentrations in the supernatant were determined using a BCA assay. Aliquots stored at –80°C were subsequently analyzed via flow cytometry to quantify multiple inflammatory mediators.

Lung Sample Collection

Following isolation, lung specimens were rinsed with 0.9% saline to remove surface blood and gently blotted dry with filter paper. Tissue samples were then processed as follows: (1) the right upper lobe was fixed in 4% paraformaldehyde; (2) the right middle lobe was weighed and oven-dried to constant weight for edema assessment; and (3) remaining tissue was immediately snap-frozen in cryovials at –80°C for subsequent analysis.

Lung W/D Weight Ratio

Freshly excised right lung parenchyma was blotted on filter paper to remove residual blood and surface moisture before determining tissue wet weight (W) using an analytical balance. Samples were subsequently desiccated at 65°C for 48 hours until constant dry weight (D) was achieved. The wet-to-dry weight ratio (W/D) was calculated as a quantitative measure of pulmonary edema severity.

Myeloperoxidase (MPO) Activity Detection

MPO enzymatic activity in lung tissues was quantified using a commercial assay kit following the manufacturer's protocol. Tissue samples were homogenized in ice-cold PBS and centrifuged at 13000 × g for 10 min at 4°C. The resulting supernatant was collected for MPO activity measurement, with absorbance readings performed as specified in the kit instructions.

Measurement of Multiple Inflammation-Related Proteins in BALF

Thirteen immune-related proteins, G-CSF, IFN γ , IL-10, IL-12, IL-17, IL-1 β , IL-2, IL-23, IL-4, IL-6, MCP-1, TNF α , and CXCL1, were quantified using the RayPlex[®] Mouse Inflammation Array kit, a bead-based multiplex immunoassay optimized for high-sensitivity detection in minimal sample volumes. Briefly, the RayPlex Multiplex Bead Cocktail and samples (or standards) were co-incubated in a 96-well plate under gentle agitation at room temperature, allowing cytokine binding to antibody-conjugated beads. Unbound proteins were removed through sequential washes, followed by sequential incubation with biotinylated detection antibodies and streptavidin-phycoerythrin conjugates to amplify fluorescence signals. Bead-associated fluorescence intensity, proportional to cytokine concentration, was analyzed via flow cytometry.

Histological Analysis

Lung tissues were placed in 4% paraformaldehyde and fully infiltrated and fixed for 24 h, and then dehydrated. After dehydration, the lung tissues were placed in xylene until transparent. The transferred lung tissues were embedded in wax, and the embedded wax blocks of lung tissues were sliced with a microtome (4 μ m thickness), placed on slides, and dried in an oven at 60°C for 40 min. Then the steps of dewaxing, rinsing, staining with hematoxylin staining solution, rinsing, soaking with eosin staining solution and rinsing were performed. After absorbing the surface water with absorbent paper, the lung tissue slides were then sequentially placed in gradient alcohol for dehydration, followed by xylene I and II for transparency, and finally the slices were sealed and placed in a warm oven for drying. The slides were placed under an inverted light microscope, and the morphological changes of the lung tissue were observed with different magnification objective lenses, and photographs were taken for preservation.

qPCR

Total RNA was extracted from collected lung tissue samples using a standardized protocol involving tissue homogenization and RNA isolation. Subsequently, RNA was reverse transcribed into cDNA for downstream analysis. Quantitative real-time PCR amplification was conducted under the following thermal cycling conditions: initial denaturation at 95°C for 30s, followed by 40 cycles of denaturation (95°C, 30s), annealing (53°C, 60s), and extension (72°C, 60s). The study evaluated the expression of tight junction-associated genes: IL-1 β (F: TGCCACCTTTTGACAGTGATG; R: TGATGTGCTGCTGCGAGATT); IL-6 (F: CCCCAATTCCAATGCTCC; R: CGCACTAGGTTTGCCGAGTA); TNF- α (F: GATCGGTC CCCAAAGGGATG; R: CCACTTGGTGGTTTGAGTG). Gene expression data were normalized to the endogenous control GAPDH (F: TGAGGCCGGTGTGAGTATGT; R: CAGTCTTCTGGGTGGCAGTGAT) and analyzed using the $2^{-\Delta\Delta Ct}$ method to determine relative expression levels.

ELISA

According to the manufacturer's protocol, standard solutions were serially diluted to generate a concentration gradient. After designating blank and sample wells, 100 μ L of either standards or test samples were added to the respective wells, followed by plate sealing and incubation. Subsequent steps included sequential reactions with primary antibody, antibody working solution, and substrate working solution. The enzymatic reaction was terminated, and absorbance was measured at 450 nm. Sample concentrations were calculated in Graphpad Prism based on the standard curve regression equation.

Immunofluorescence

Paraffin-embedded tissue sections were dewaxed, rehydrated, and washed with pure water (10 min, twice). After removing excess liquid, endogenous peroxidase activity was blocked by incubating the sections with 3% H₂O₂ in a humidified chamber for 10 min, followed by three 5-min washes with TBST. Antigen retrieval was performed in preheated 1 \times EDTA buffer (pH 9.0) using microwave heating (95°C for 3 min, then maintained for 10 min), followed by natural cooling to room temperature. After three additional TBST washes (5 min each), nonspecific binding was blocked with 5% BSA for 2 h at room temperature. The sections were then incubated with primary antibody at 4°C overnight. After warming to room temperature, the slides were washed three times with TBST (5 min each), and species-matched fluorescent secondary antibody was applied, followed by incubation at 37°C for 1 h in the dark box. After removing the secondary antibody, nuclei were counterstained with DAPI (5 min), followed by three 10-min TBST washes. Finally, the slides were mounted with an anti-fade mounting medium and imaged using a confocal microscope (Leica SP8).

Western Blot

Protein expression in lung tissue was examined by Western blot. Briefly, lung tissues were homogenized in RIPA lysis buffer containing protease and phosphatase inhibitors and incubated on ice for 30 min. Lysates were centrifuged at 12,000 \times g for 15 min at 4 °C, and supernatants were collected. Protein concentrations were determined using a BCA protein assay kit. Equal amounts of protein (20 μ g) were separated on SDS-polyacrylamide gradient gels (5–20%) and transferred to PVDF membranes. Membranes were blocked with 5% non-fat dry milk in TBST for 1 h at room temperature and then incubated overnight at 4 °C with primary antibodies against NLRP3, cleaved caspase-1, cleaved GSDMD, p-NF- κ B, IL-1 β , IL-18, and β -actin (all diluted at 1:1000). After washing, membranes were incubated with HRP-conjugated secondary antibodies for 1 h at room temperature. Protein bands were visualized using enhanced chemiluminescence and imaged with a Chemiluminescence system. Band intensities were quantified using ImageJ software and normalized to β -actin.

Flow Cytometry

Pyroptotic cell death in lung tissue was assessed by flow cytometry using an Annexin V-CoraLite 488/propidium iodide (PI) detection kit (Proteintech, Cat. No. PF00005). Briefly, lung tissues were digested with collagenase and DNase I to generate single-cell suspensions, which were filtered through a 70- μ m mesh and washed twice with cold PBS. Cells were resuspended in 100 μ L of 1 \times binding buffer, followed by incubation with 5 μ L of Annexin V-CoraLite 488 and 5 μ L of PI for 10 min at room temperature in the dark. After incubation, 400 μ L of binding buffer was added, and samples were immediately analyzed

on a flow cytometer using 488 nm excitation and FITC and PI detection channels. Single-stained controls were included for compensation adjustment. Data were processed with FlowJo software. Cells were classified as pyroptotic (Annexin V+/PI+) in Q2.²⁰ The proportion of Annexin V+/PI+ cells was quantified to represent pyroptotic cell death.

Transmission Electron Microscope (TEM)

Freshly isolated lung tissue fragments (1 mm³) were promptly fixed in 2.5% glutaraldehyde at 4°C for 24 h. After primary fixation, specimens were washed three times (15 min each) in PBS to remove excess fixative, followed by post-fixation in 1% osmium tetroxide (OsO₄) for 2 h at room temperature. Residual OsO₄ was eliminated via three 15-min rinses in 0.1 M phosphate buffer. Dehydration was carried out using an ascending acetone series (30%, 50%, 70%, 80%, and 95%, 10 min per step), followed by two 20-min incubations in absolute acetone. Tissues were then infiltrated and embedded in pure EMBed 812 resin. Polymerization was conducted at 60°C for a minimum of 48 h. Ultra-thin sections (70 nm) were obtained using an ultramicrotome, mounted on copper grids, and sequentially stained with uranyl acetate (10 min) and lead citrate (10 min). Finally, samples were examined under a transmission electron microscope operated at 80 kV, and images were acquired using a CCD camera.

Statistical Analyses

Results are expressed as mean ± SEM. Following verification of normal distribution using the Kolmogorov–Smirnov test, intergroup differences were assessed by one-way ANOVA with Tukey's test for multiple comparisons. Non-parametric datasets such as histological scores were used Kruskal–Wallis with Dunn's test, with statistical significance set at $p < 0.05$.

Results

P2Y₁₂R Antagonists Attenuated LPS-induced Inflammatory Response and Reversed ALI in Mice

The histological analysis of lung tissue (Figure 1A) in the control group showed normal lung architecture with well-defined alveolar spaces and intact alveolar walls. No evidence of inflammation, edema, or tissue damage was observed in these mice. In the ALI group, significant histopathological alterations were evident. At both 20x and 63x magnifications, there was pronounced inflammatory infiltration in the lung parenchyma, particularly around the alveolar spaces. The alveolar walls were markedly thickened, and the alveolar cavities were reduced in size. There was also noticeable edema in the interstitial spaces, and several areas exhibited disrupted epithelial cells. These findings are indicative of ALI induced by LPS, with evident damage to the lung tissue structure. In the Ticagrelor-treated group, lung histology showed a noticeable improvement. Although mild inflammation was still present, the alveolar walls appeared less thickened, and the overall lung architecture was better preserved compared to the ALI group. The inflammatory cells in the alveolar spaces were reduced, and the alveolar cavities appeared more open. Similarly, in the Prasugrel-treated group, the lung tissue exhibited moderate improvement, with a reduction in alveolar wall thickening and inflammatory cell infiltration. In the Clopidogrel-treated group, some recovery in lung structure was observed, though less pronounced compared to Ticagrelor and Prasugrel. Mild inflammatory infiltration and alveolar wall thickening persisted, but the overall lung structure was still more preserved compared to the ALI group. The quantitative results indicated that Clopidogrel, Prasugrel, and Ticagrelor could decrease the histological score in mice treated by LPS (Figure 1B). These histological findings suggested that P2Y₁₂R antagonists, particularly Ticagrelor, alleviated LPS-induced lung injury by reducing inflammation, alveolar damage, and preserving lung architecture.

Quantitative analysis of lung injury was assessed by the lung wet/dry ratio (Figure 1C), which was significantly increased in the ALI group compared to the control group, indicating elevated pulmonary edema. Treatment with Clopidogrel, Prasugrel, and Ticagrelor significantly reduced the wet/dry ratio, with Ticagrelor showing the most prominent effect ($p < 0.01$). Protein levels in BALF (Figure 1D) were also significantly elevated in the ALI group, reflecting an inflammatory response. Treatment with Clopidogrel, Prasugrel, and Ticagrelor resulted in decreased protein concentrations in BALF, with Ticagrelor showing the greatest reduction ($p < 0.001$). MPO activity, a marker of neutrophil infiltration (Figure 1E), was significantly increased in the

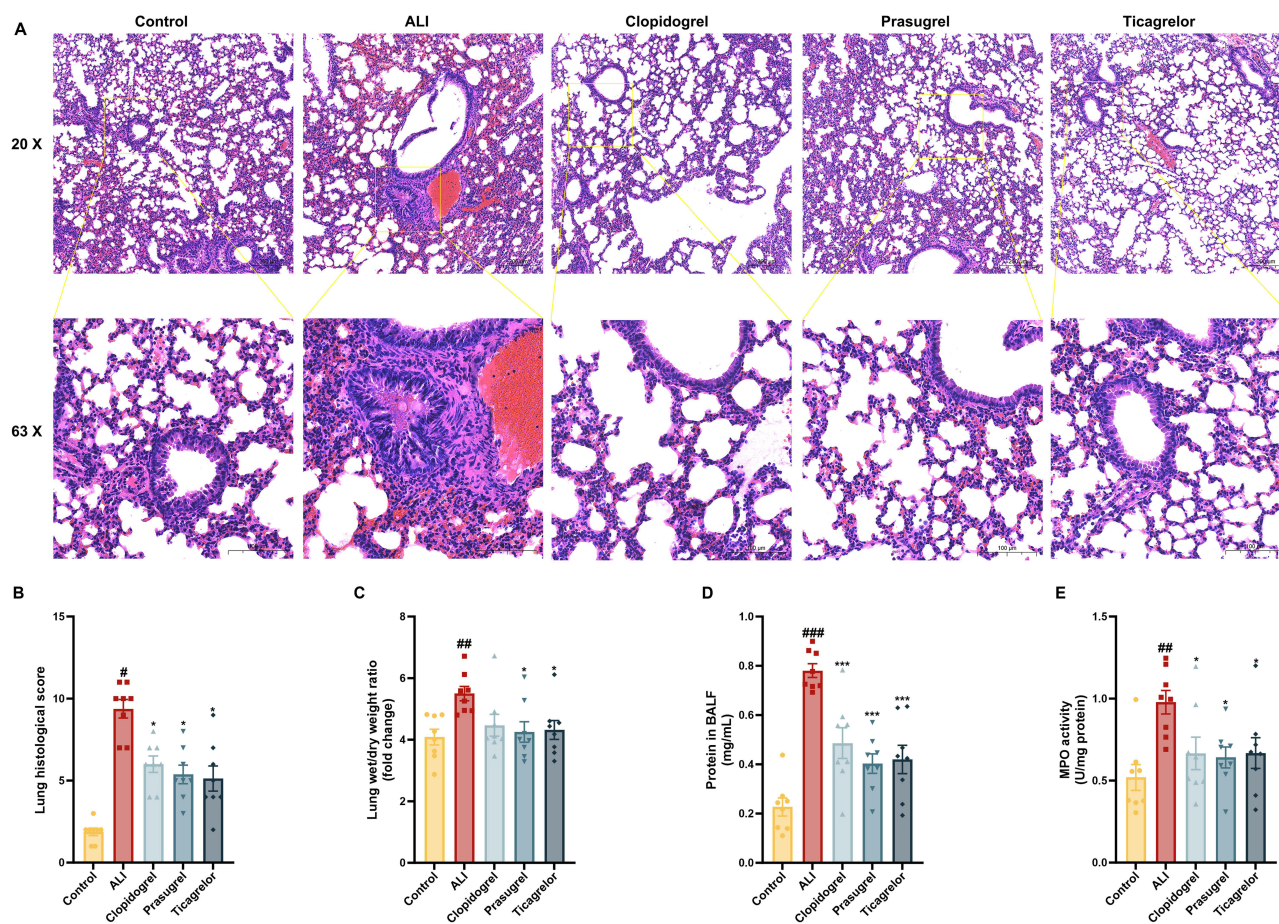


Figure 1 Effects of P2Y₁₂R (P2Y₁₂R) antagonists on lipopolysaccharide (LPS)-induced acute lung injury (ALI). **(A)** Representative H&E-stained lung sections at 20x and 63x magnifications. Scale bars represent 100 μ m (20x) and 50 μ m (63x). **(B)** Lung histological score. **(C)** Lung wet/dry ratio. **(D)** Protein concentration in bronchoalveolar lavage fluid (BALF). **(E)** Myeloperoxidase (MPO) activity. Data were expressed as mean \pm SEM, n = 8. #p < 0.05, ##p < 0.01 and ###p < 0.001 vs control, *p < 0.05 and ***p < 0.001 vs ALI.

ALI group. Treatment with Clopidogrel, Prasugrel, and Ticagrelor led to reduced MPO activity, with Ticagrelor again showing the most substantial reduction ($p < 0.01$).

Together, these results demonstrate that P2Y₁₂R antagonists, particularly Ticagrelor, mitigate lung injury and inflammation in the LPS-induced ALI model.

P2Y₁₂R Antagonists Regulated Cytokine and Chemokine Levels in BALF in LPS-Induced ALI

To further evaluate the inflammatory response in LPS-induced ALI, the levels of various cytokines and chemokines including IL-1 β (Figure 2A), IL-2 (Figure 2B), IL-4 (Figure 2C), IL-6 (Figure 2D), IL-10 (Figure 2E), IL-12 (Figure 2F), IL-17 (Figure 2G), IL-23 (Figure 2H), TNF- α (Figure 2I), INF- γ (Figure 2J), G-CSF (Figure 2K), CXCL-1 (Figure 2L), and MCP-1 (Figure 2M) were measured in BALF.

The pro-inflammatory cytokine IL-1 β (Figure 2A) was significantly elevated in the ALI group compared to the control group ($p < 0.01$). Treatment with Clopidogrel, Prasugrel, and Ticagrelor significantly reduced IL-1 β levels, with Ticagrelor showing the most substantial reduction ($p < 0.001$). IL-2 (Figure 2B) and IL-12 (Figure 2F) were also significantly increased in the ALI group, and all treatment groups showed reduced IL-2 and IL-12 levels.

The levels of anti-inflammatory cytokines such as IL-10 (Figure 2E) were notably decreased in the ALI group, but all P2Y₁₂R antagonists restored IL-10 levels. Ticagrelor treatment showed the most prominent effect ($p < 0.01$). IL-6 (Figure 2D), a key mediator of inflammation, was significantly elevated in the ALI group ($p < 0.01$) and was reduced by

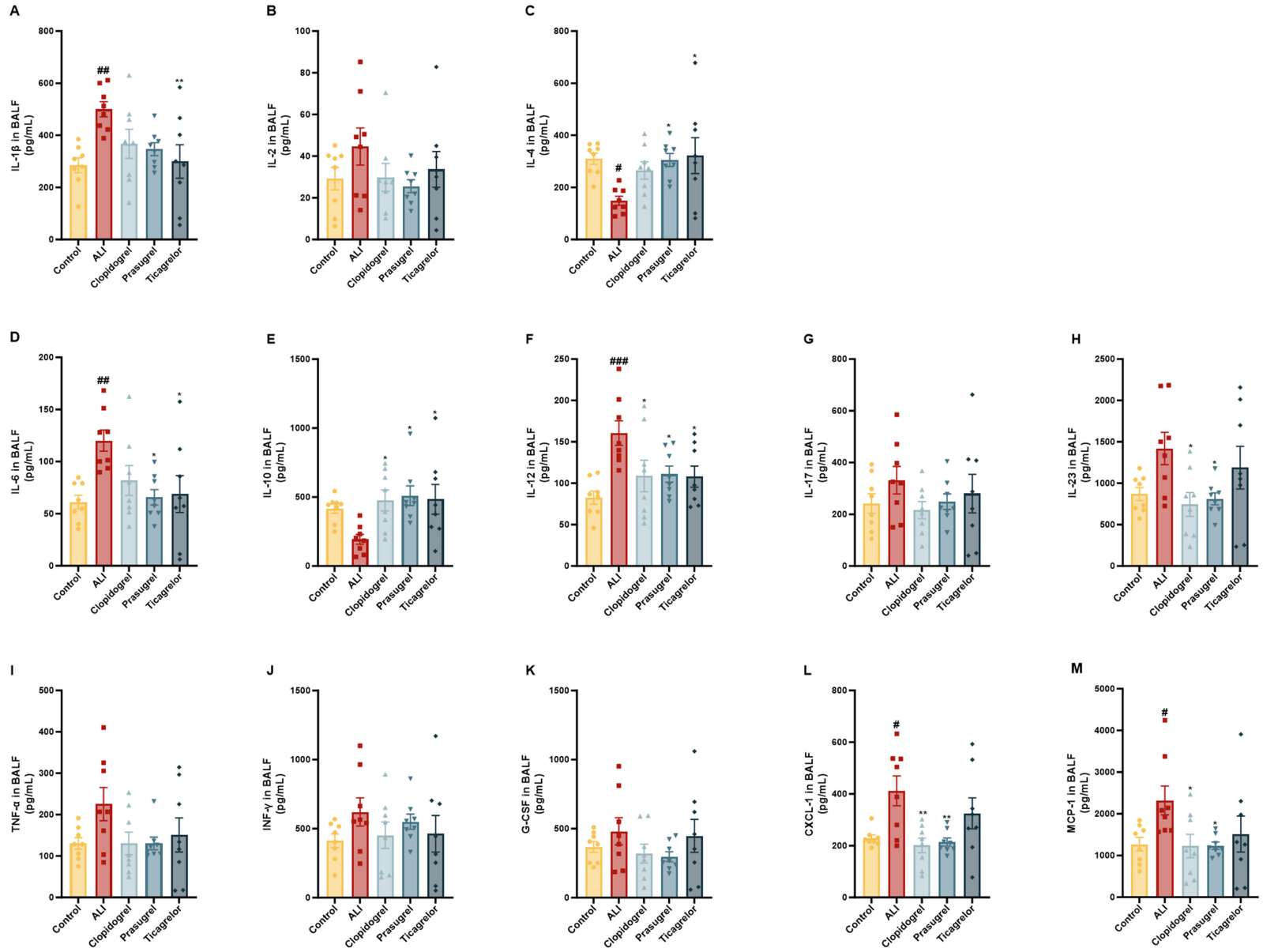


Figure 2 Cytokine and chemokine levels in bronchoalveolar lavage fluid (BALF) in lipopolysaccharide (LPS)-induced acute lung injury (ALI) after treatment with P2Y₁₂R antagonist. (A) IL-1 β , (B) IL-2, (C) IL-4, (D) IL-6, (E) IL-10, (F) IL-12, (G) IL-17, (H) IL-23, (I) TNF- α , (J) INF- γ , (K) G-CSF, (L) CXCL-1, and (M) MCP-1. Data were expressed as mean \pm SEM, n = 8. #p < 0.05, ##p < 0.01 and ###p < 0.001 vs control, *p < 0.05 and **p < 0.01 vs ALI.

Ticagrelor and Prasugrel treatments, particularly Ticagrelor ($p < 0.001$). The levels of IL-4 (Figure 2C), and IL-17 (Figure 2G) did not show significant differences between the ALI and treatment groups. However, IL-23 (Figure 2H), a cytokine involved in Th17 cell differentiation, was significantly elevated in the ALI group compared to the control. All treatments, particularly Ticagrelor, significantly reduced IL-23 levels ($p < 0.01$).

TNF- α (Figure 2I), a major pro-inflammatory cytokine, was significantly elevated in the ALI group and was reduced by Ticagrelor and Prasugrel treatments ($p < 0.05$). INF- γ (Figure 2J), another pro-inflammatory cytokine, followed a similar trend, with Ticagrelor and Prasugrel showing significant reductions compared to the ALI group ($p < 0.05$).

The chemokines CXCL-1 (Figure 2L) and MCP-1 (Figure 2M), involved in neutrophil recruitment, were significantly elevated in the ALI group and were significantly reduced by Ticagrelor and Prasugrel treatments ($p < 0.05$). G-CSF (Figure 2K), a growth factor involved in neutrophil production, was also significantly increased in the ALI group and reduced by Ticagrelor and Prasugrel ($p < 0.01$).

These results suggest that P2Y₁₂R antagonists, particularly Ticagrelor, reduce the levels of pro-inflammatory cytokines and chemokines in the LPS-induced ALI model, providing evidence of their anti-inflammatory effects.

P2Y₁₂R Antagonists Decreased Gene Expression and Protein Levels in Lung Tissues

To investigate the inflammatory response at both the mRNA and protein levels, we measured gene expression and protein concentrations for IL-1 β , IL-6, and TNF- α in lung tissues.

IL-1 β (Figure 3A) gene expression was significantly elevated in the ALI group compared to the control group ($p < 0.001$). Treatment with Clopidogrel, Prasugrel, and Ticagrelor significantly reduced IL-1 β mRNA levels, with Ticagrelor showing the most pronounced effect. Similarly, IL-6 (Figure 3B) gene expression was markedly increased in the ALI group ($p < 0.01$), and Prasugrel, and Ticagrelor treatment significantly downregulated IL-6 gene expression ($p < 0.05$, $p < 0.05$, respectively). TNF- α (Figure 3C) gene expression was also significantly elevated in the ALI group, and treatment with Clopidogrel, Prasugrel, and Ticagrelor significantly reduced its expression ($p < 0.05$, $p < 0.01$, $p < 0.001$, respectively).

In addition to mRNA expression, we also measured IL-1 β , IL-6, and TNF- α protein levels in lung tissue. IL-1 β (Figure 3D), IL-6 (Figure 3E), and TNF- α (Figure 3F) protein levels in lung tissue were significantly elevated in the ALI group compared to the control group. Treatment with Clopidogrel, Prasugrel, and Ticagrelor significantly reduced these protein levels in lung tissues. Ticagrelor was particularly effective in reducing the expression of these pro-inflammatory cytokines in the lung tissue, with reductions reaching statistical significance ($p < 0.001$ for IL-1 β and IL-6, $p < 0.05$ for TNF- α).

These results indicate that P2Y₁₂R antagonists, particularly Ticagrelor, reduce both the gene expression and protein levels of key pro-inflammatory cytokines in lung tissues, suggesting that they effectively modulate the inflammatory response in lung.

Effects of P2Y₁₂R Antagonists on the Expression of TLR4, P2Y₁₂R, and pNF- κ B in Lung Tissue

We next examined the expression of TLR4, P2Y₁₂R, and pNF- κ B in lung tissue using immunofluorescence staining. In the ALI group, TLR4 expression (Figure 4A and B) was significantly increased compared to the control group ($p < 0.01$). Treatment with Clopidogrel, Prasugrel, and Ticagrelor did not significantly change the expression of TLR4. In addition, P2Y₁₂R expression (Figure 4C and D) was partly increased in the ALI group. All treatments did not reduce P2Y₁₂R expression. Further, the activation of NF- κ B was assessed by measuring the phosphorylation of NF- κ B (pNF- κ B) in lung tissue (Figure 4E and F). pNF- κ B levels were significantly elevated in the ALI group compared to the control ($p < 0.001$). Clopidogrel, Prasugrel, and Ticagrelor treatment all significantly reduced pNF- κ B expression, with Ticagrelor exhibiting the most significant reduction ($p < 0.001$).

On the other hand, Western blot (Figure 5A) indicated that although LPS did not significantly increase the levels of TLR4 (Figure 5B), P2Y₁₂R (Figure 5C), and pNF- κ B levels (Figure 5D), Clopidogrel, Prasugrel, and Ticagrelor treatment could inhibited that activation of NF- κ B signaling (Figure 5).

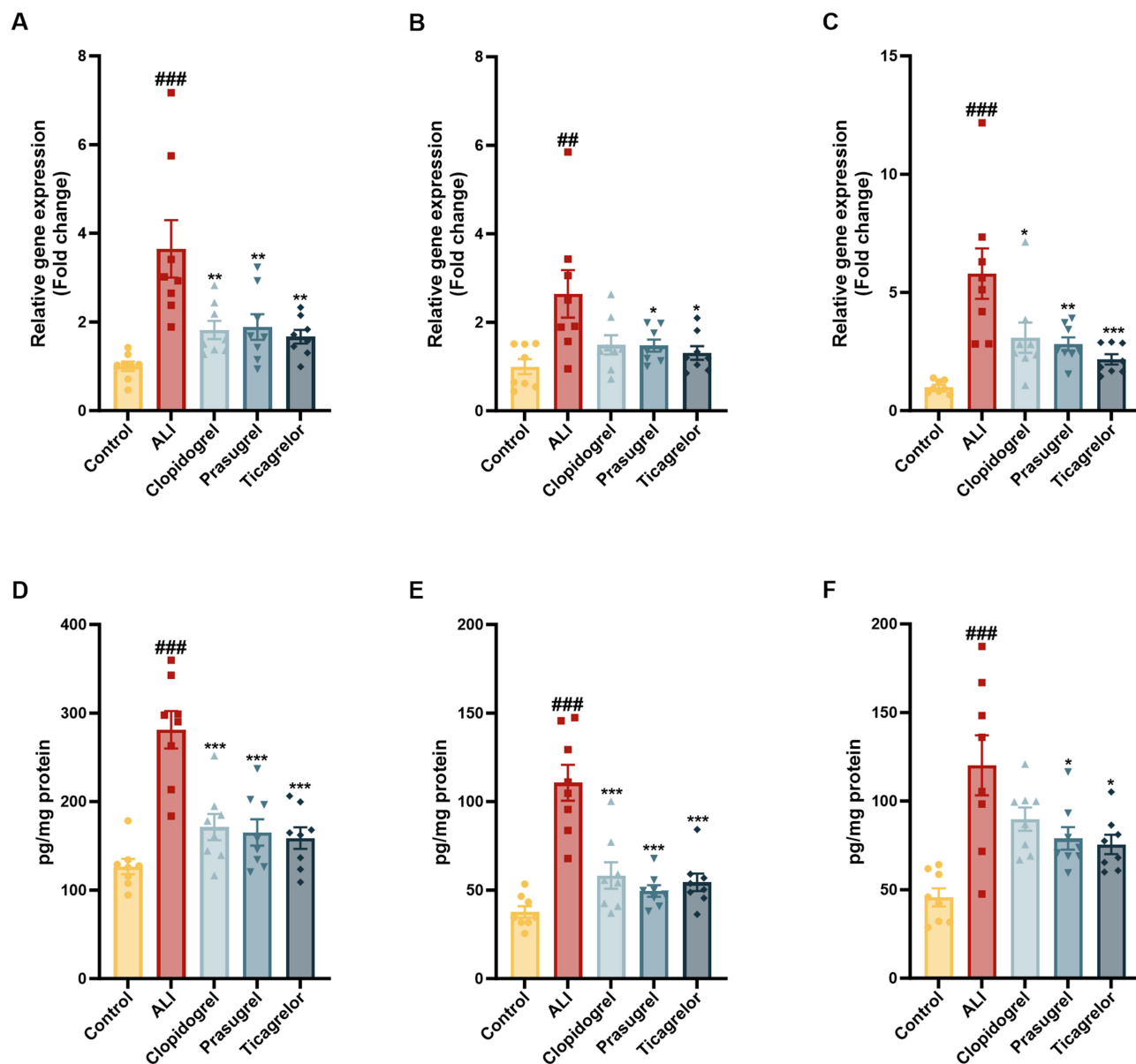


Figure 3 Gene expression and protein levels of pro-inflammatory cytokines in lung tissue in response to P2Y12 receptor (P2Y12R) antagonists. (A) IL-1 β gene expression by qPCR, (B) IL-6 gene expression by qPCR, (C) TNF- α gene expression by qPCR, (D) IL-1 β protein by ELISA, (E) IL-6 protein by ELISA, (F) TNF- α protein by ELISA. Data were expressed as mean \pm SEM, n = 8. ###p < 0.001 and ####p < 0.001 vs control, *p < 0.05, **p < 0.01 and ***p < 0.001 vs acute lung injury (ALI).

These results suggest that P2Y12R antagonists attenuate the activation of NF- κ B in lung tissue, potentially contributing to their anti-inflammatory effects in LPS-induced ALI.

Effects of P2Y12R Antagonists on the NLRP3, ASC, Caspase-1, and GSDMD in Lung Tissue

To further investigate the mechanisms underlying pyroptosis in LPS-induced ALI, we evaluated the expression of key inflammasome components, including NLRP3, ASC, Caspase-1, and GSDMD, using immunofluorescence staining and Western blot.

In the ALI group, NLRP3 (Figure 6A and B) expression was significantly increased compared to the control group ($p < 0.001$). Treatment with Clopidogrel, Prasugrel, and Ticagrelor significantly reduced NLRP3 expression, with Clopidogrel showing the most substantial effect ($p < 0.001$). ASC (Figure 6C and D), another critical component of

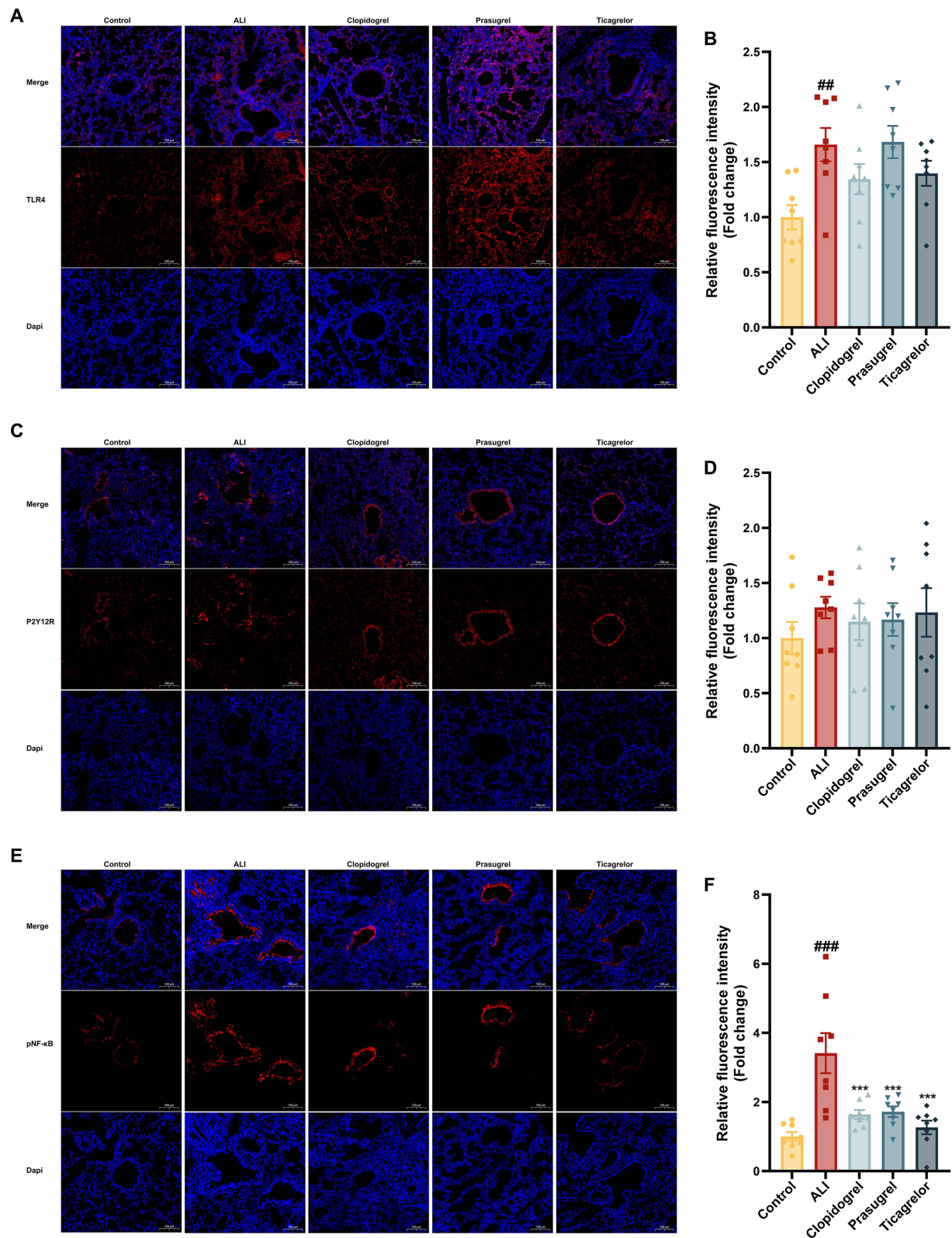


Figure 4 Expression of TLR4, P2Y12 receptor (P2Y12R), and pNF- κ B in lung tissue in response to P2Y12R antagonists. **(A)** Representative immunofluorescence staining of TLR4, **(C)** P2Y12R, and **(E)** pNF- κ B in lung tissue sections. The expression of each protein is shown in red, with nuclei stained blue using DAPI. Scale bars represent 100 μ m. **(B)** Relative fluorescence intensity of TLR4, **(D)** P2Y12R, and **(F)** pNF- κ B in lung tissue. Data were expressed as mean \pm SEM, $n = 8$. ^{##} $p < 0.01$ and ^{###} $p < 0.001$ vs control, ^{***} $p < 0.001$ vs acute lung injury (ALI).

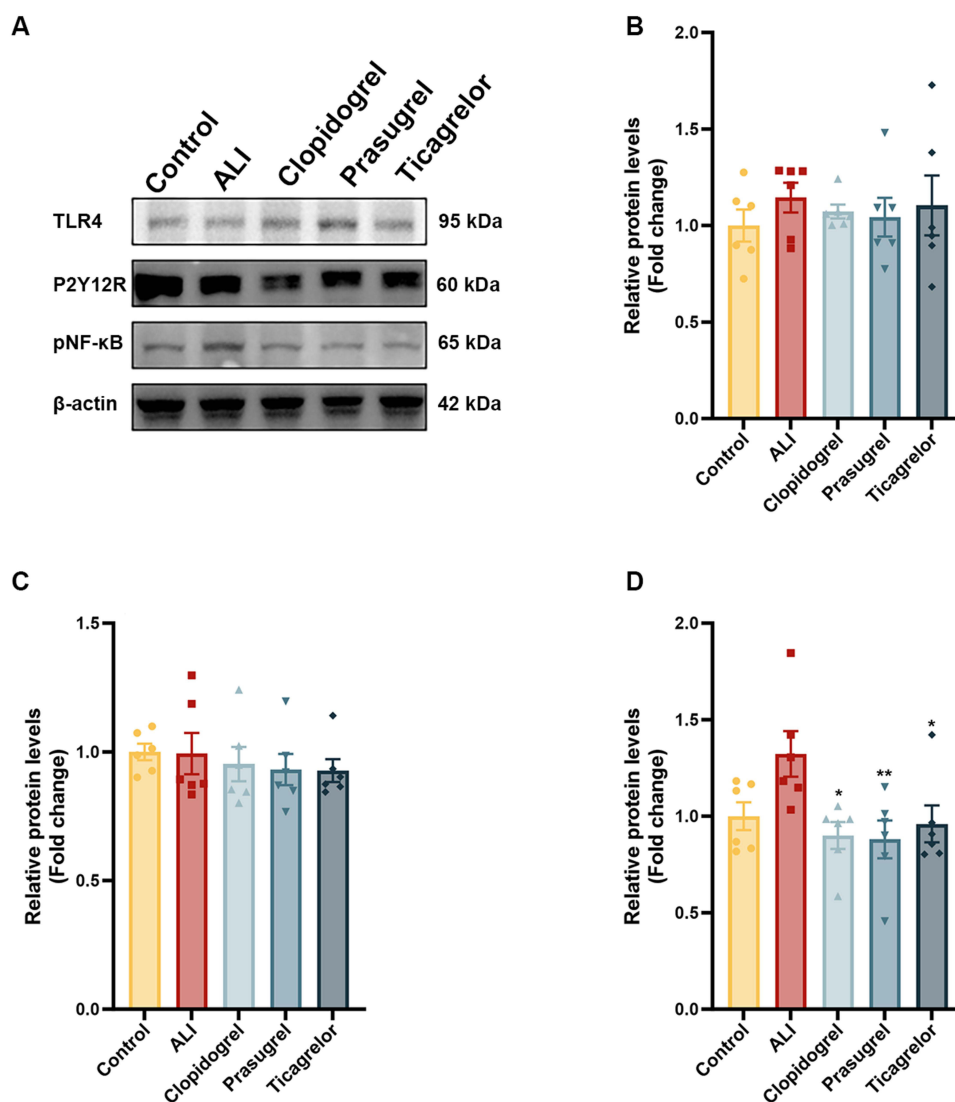


Figure 5 The effects of P2Y12 receptor (P2Y12R) antagonist on the levels of TLR4, P2Y12R, and pNF- κ B in lung tissue. **(A)** Representative blots of TLR4, P2Y12R, and pNF- κ B. Relative levels of **(B)** TLR4, **(C)** P2Y12R, and **(D)** pNF- κ B in response to P2Y12R antagonists. Data were expressed as mean \pm SEM, $n = 6$. * $p < 0.05$ and ** $p < 0.01$ vs acute lung injury (ALI).

the inflammasome, was also significantly upregulated in the ALI group ($p < 0.001$). Clopidogrel, Prasugrel, and Ticagrelor treatment led to significant reductions in ASC expression. Caspase-1 (Figure 6E and F) and GSDMD (Figure 6G and H) are key proteins involved in pyroptosis, and both were significantly elevated in the ALI group compared to the control. Treatment with Clopidogrel, Prasugrel, and Ticagrelor significantly reduced the expression of both Caspase-1 and GSDMD in lung tissues.

On the other hand, Western blot (Figure 7A) was performed to detect the levels of NLRP3 (Figure 7B), Cleaved Caspase-1 (Figure 7C), Cleaved GSDMD (Figure 7D), pro GSDMD (Figure 7E), mature IL-1 β (Figure 7F), pro IL-1 β (Figure 7G), mature IL-18 (Figure 7H), and pro IL-18 (Figure 7I) in lung. The data indicated that LPS increased the levels of NLRP3, cleaved Caspase-1, cleaved GSDMD, and mature IL-18 in lung tissue, although there was no significant increase of mature IL-1 β levels. On the contrary, treatment with Ticagrelor significantly decreased the levels of NLRP3, cleaved Caspase-1, cleaved GSDMD, mature IL-1 β , and mature IL-18 levels. Treatment with Prasugrel significantly decreased the levels of NLRP3, cleaved Caspase-1, mature IL-1 β , and mature IL-18 levels. Treatment with Clopidogrel significantly decreased the levels of NLRP3 and mature IL-18 levels.

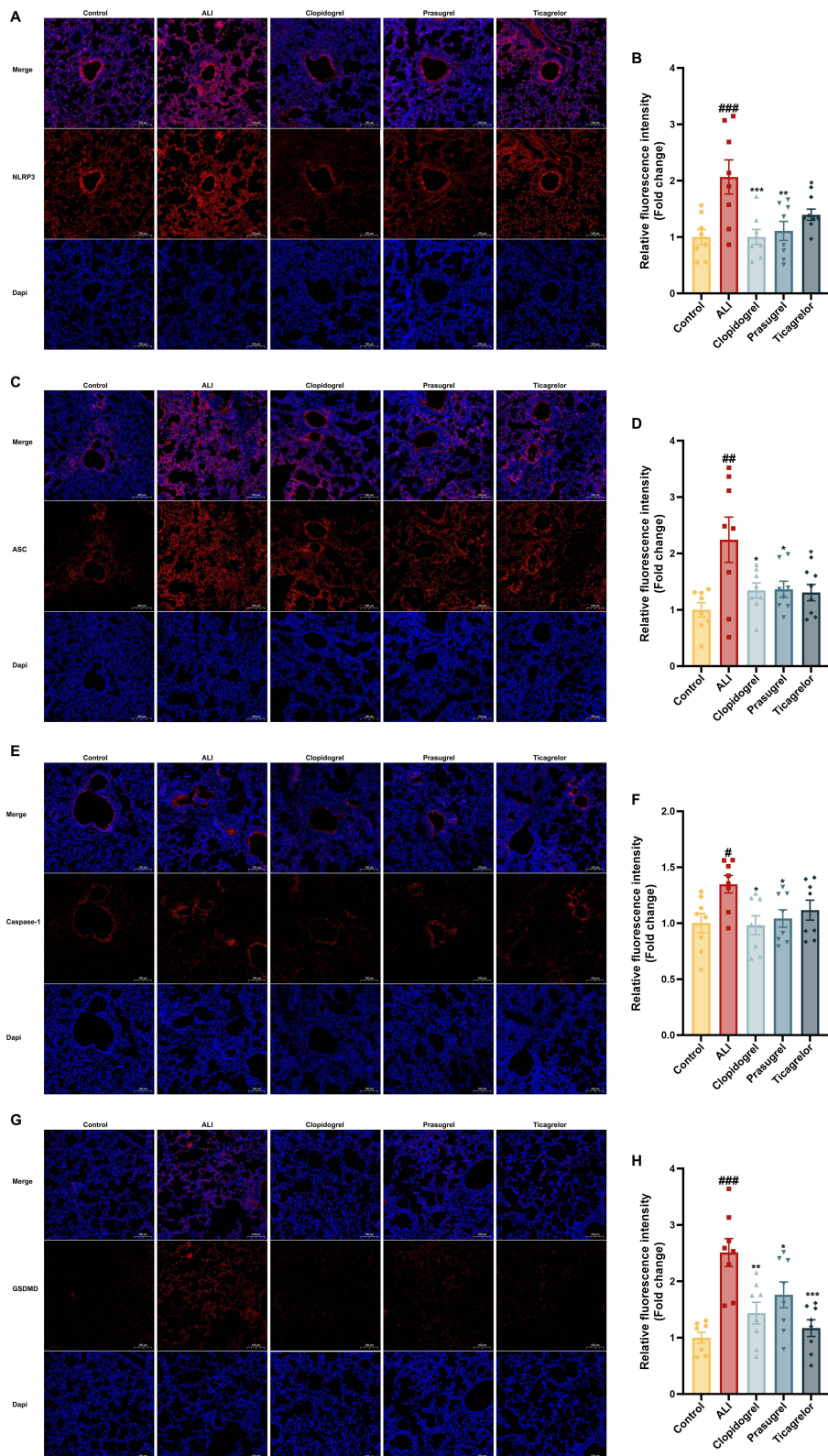


Figure 6 Expression of NLRP3, ASC, Caspase-1, and gasdermin D (GSDMD) in lung tissue in response to P2Y12 receptor (P2Y12R) antagonists. **(A)** Representative immunofluorescence staining of NLRP3, **(C)** ASC, **(E)** Caspase-1, and **(G)** GSDMD in lung tissue sections. The expression of each protein was shown in red, with nuclei stained blue using DAPI. Scale bars represent 100 μ m. **(B)** Relative fluorescence intensity of NLRP3, **(D)** ASC, **(F)** Caspase-1, and **(H)** GSDMD in lung tissue. Data were expressed as mean \pm SEM, n = 8. #p < 0.05, ###p < 0.01 and ####p < 0.001 vs control, *p < 0.05, **p < 0.01 and ***p < 0.001 vs acute lung injury (ALI).

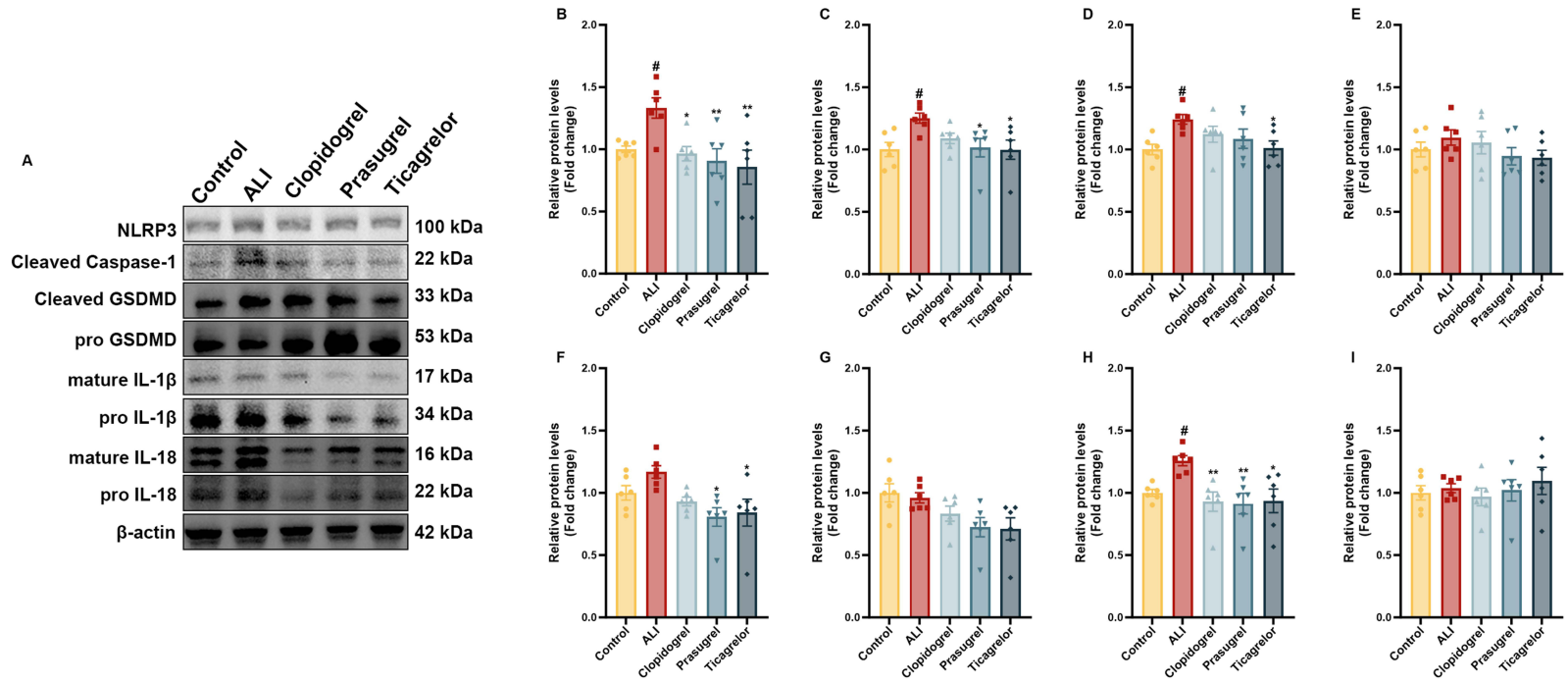


Figure 7 The attenuated effects of P2Y₁₂ receptor (P2Y₁₂R) antagonist on the activation of NLRP3/Caspase-1/gasdermin D (GSDMD) signaling pathway in lung tissue. **(A)** Representative blots. Relative levels of **(B)** NLRP3, **(C)** Cleaved Caspase-1, **(D)** Cleaved GSDMD, **(E)** pro GSDMD, **(F)** mature IL-1 β , **(G)** pro IL-1 β , **(H)** mature IL-18, and **(I)** pro IL-18 in response to P2Y₁₂R antagonists. Data were expressed as mean \pm SEM, n = 6. [#]p < 0.05 vs control, ^{*}p < 0.05 and ^{**}p < 0.01 vs acute lung injury (ALI).

These results demonstrate that P2Y₁₂R antagonists reduce the expression of key components of the inflammasome and pyroptosis pathway in lung tissue, suggesting their potential to alleviate pyroptosis in LPS-induced ALI.

P2Y₁₂R Antagonists Decreased Pyroptotic Cell Death in Lung Tissue

To explore the quantitative data for pyroptotic cell by P2Y₁₂R antagonists, pyroptotic rate in lung tissue was assessed by flow cytometry using an Annexin V-CoraLite 488/PI kit (Figure 8A–E). Pyroptosis was defined as Annexin V+/PI+. Flow cytometry indicated a significantly increased ratio of pyroptotic rate in the LPS groups (Figure 8F). However, Clopidogrel and Ticagrelor significantly reduced pyroptotic cell death. Prasugrel tended to decrease pyroptotic rate ($p = 0.05$). These results confirmed that P2Y₁₂R antagonist could inhibit pyroptosis in LPS-induced ALI.

Ultrastructural Analysis of Lung Tissue Using Transmission Electron Microscopy in Response to P2Y₁₂R Antagonists

The TEM images revealed distinct ultrastructural alterations in lung tissues from control mice, LPS-induced ALI mice, and those treated with Clopidogrel, Prasugrel, and Ticagrelor. The images are taken at different magnifications (4000X, 10000X, and 30000X) to provide a detailed view of cellular changes.

In the Control group (Figure 9A), the cellular ultrastructure was well-preserved, with normal alveolar epithelial cells exhibiting intact membranes and clearly defined organelles. The mitochondria were of regular shape, with dense cristae and intact membranes. The rough endoplasmic reticulum appeared regular without dilation or damage. The cellular integrity was maintained, with no noticeable signs of inflammation or injury.

In the LPS-induced ALI group (Figure 9B), significant cellular damage was observed. The alveolar epithelial cells showed signs of swelling, with mitochondria appearing enlarged and exhibiting vacuolation. The endoplasmic reticulum displayed dilation and signs of stress, such as membrane disruption and ribosome detachment. The cytoplasm contained vacuoles, indicative of severe cellular injury. These findings indicated the acute inflammatory response caused by LPS exposure, leading to cellular dysfunction and organelle damage.

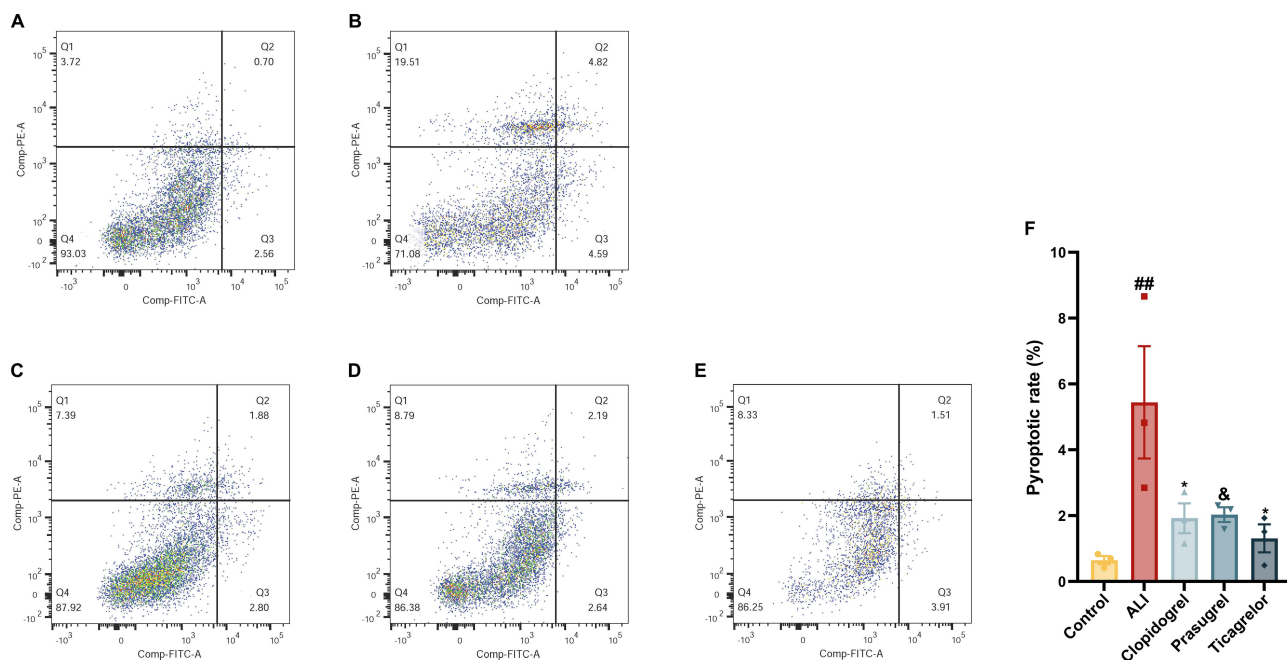


Figure 8 P2Y₁₂ receptor (P2Y₁₂R) antagonists reduced the percentage of pyroptotic cell death. Representative image of flow cytometry from (A) Control, (B) ALI, (C) Clopidogrel, (D) Prasugrel, and (E) Ticagrelor. (F) Flow cytometry quantification of pyroptotic population. Lung cells from fresh tissue were assessed for pyroptosis using flow cytometry based on CoraLite Plus 488-Annexin V and propidium iodide (PI) staining. Pyroptosis was defined as Annexin V+/PI+. Data were expressed as mean \pm SEM, $n = 3$. ## $p < 0.01$ vs control, * $p < 0.05$ vs ALI, $\delta p = 0.05$ vs acute lung injury (ALI).

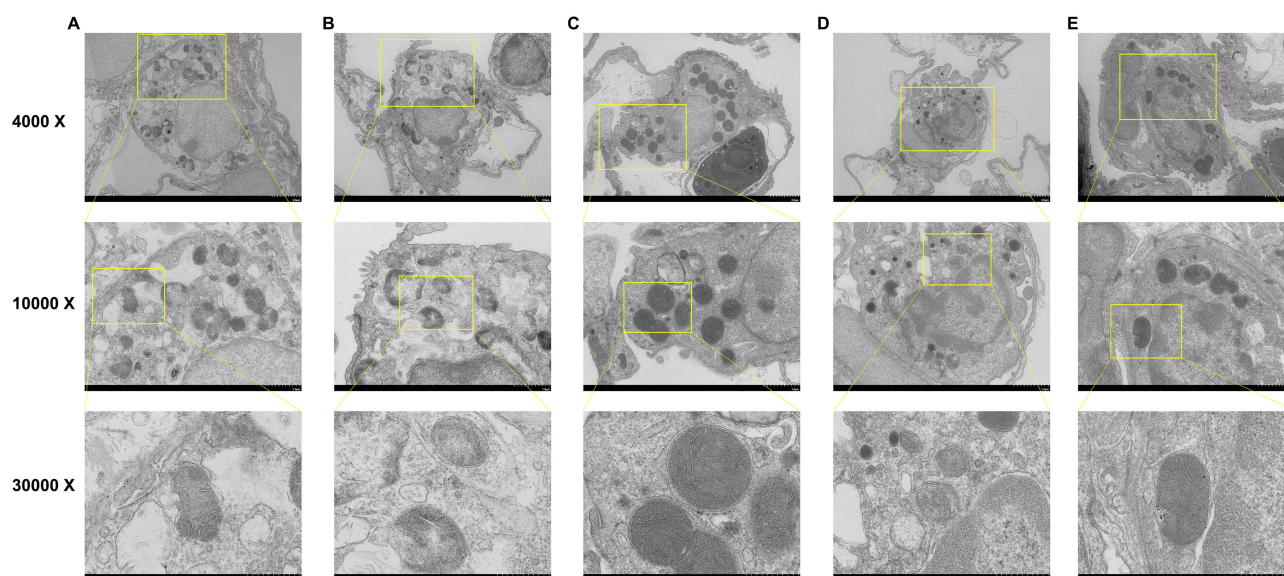


Figure 9 Ultrastructural analysis of lung tissue using transmission electron microscopy (TEM) in response to P2Y12 receptor (P2Y12R) antagonists. **(A)** Control group showing normal lung cell ultrastructure with intact organelles. **(B)** Acute lung injury (ALI) group showing severe ultrastructural damage, including mitochondrial swelling and membrane disintegration. **(C)** Clopidogrel-treated group showing mild improvement but some residual cellular damage. **(D)** Prasugrel-treated group showing moderate recovery in lung cell ultrastructure. **(E)** Ticagrelor-treated group showing some preservation of mitochondrial structure and less cellular damage. TEM images are shown at 4000x, 10000x (the enlarged area of yellow box in 4000x images), and 30000x (the enlarged area of yellow box in 10000x images) magnifications. Scale bars: 2 μm (4000x), 1 μm (10000x), 0.5 μm (30000x).

The Clopidogrel-treated group (Figure 9C) showed ultrastructural features similar to the Ticagrelor group, with relatively preserved mitochondrial morphology and less cytoplasmic vacuolization. The endoplasmic reticulum appeared less dilated compared to the LPS group, and organelles maintained a more organized structure. The Clopidogrel treatment seemed to provide moderate protection against LPS-induced damage, similar to Ticagrelor.

In the Prasugrel-treated group (Figure 9D), the cellular ultrastructure showed moderate protection from LPS-induced damage. The mitochondria remained more intact than in the LPS group, although some mild swelling and vacuolization were still observed. The endoplasmic reticulum appeared somewhat dilated, but the extent of damage was less than in the ALI group. The overall cellular integrity was improved, suggesting that Prasugrel may offer a protective effect, though not as pronounced as Ticagrelor.

The Ticagrelor-treated group (Figure 9E) exhibited a reduction in the extent of cellular damage compared to the LPS group. Mitochondria appeared less swollen, with relatively preserved cristae. While some swelling was still evident, particularly in the endoplasmic reticulum, the overall ultrastructure suggests that Ticagrelor may provide partial protection against LPS-induced cellular injury. There was less vacuolization in the cytoplasm, and the organelles appeared less disrupted.

Discussion

In this study, we investigated the protective effects of three clinically available P2Y12R antagonists, Clopidogrel, Prasugrel, and Ticagrelor, on LPS-induced ALI in mice. Our findings demonstrated that P2Y12R blockade ameliorated LPS-induced lung damage, reduced pro-inflammatory cytokine production, and attenuated pyroptosis by downregulating the NF- κ B/NLRP3/GSDMD signaling axis. In detail, pyroptosis proceeds through a two-signal pathway, firstly, LPS triggers TLR4 primes NF- κ B-dependent transcription of pro-IL-1 β and NLRP3, while NLRP3 activation promotes caspase-1 cleavage of GSDMD and maturation/release of IL-1 β and IL-18. In the present study, P2Y12R antagonists attenuated both signals, reducing pNF- κ B, NLRP3/ASC/caspase-1/GSDMD, and suppressing release of both IL-1 β and IL-18, providing direct evidence for inhibition of the canonical inflammasome-driven pyroptotic cascade (Figure 10). Among the tested agents, Ticagrelor exhibited the most potent protective effects, suggesting its potential as a candidate for repurposing in the treatment of ALI.

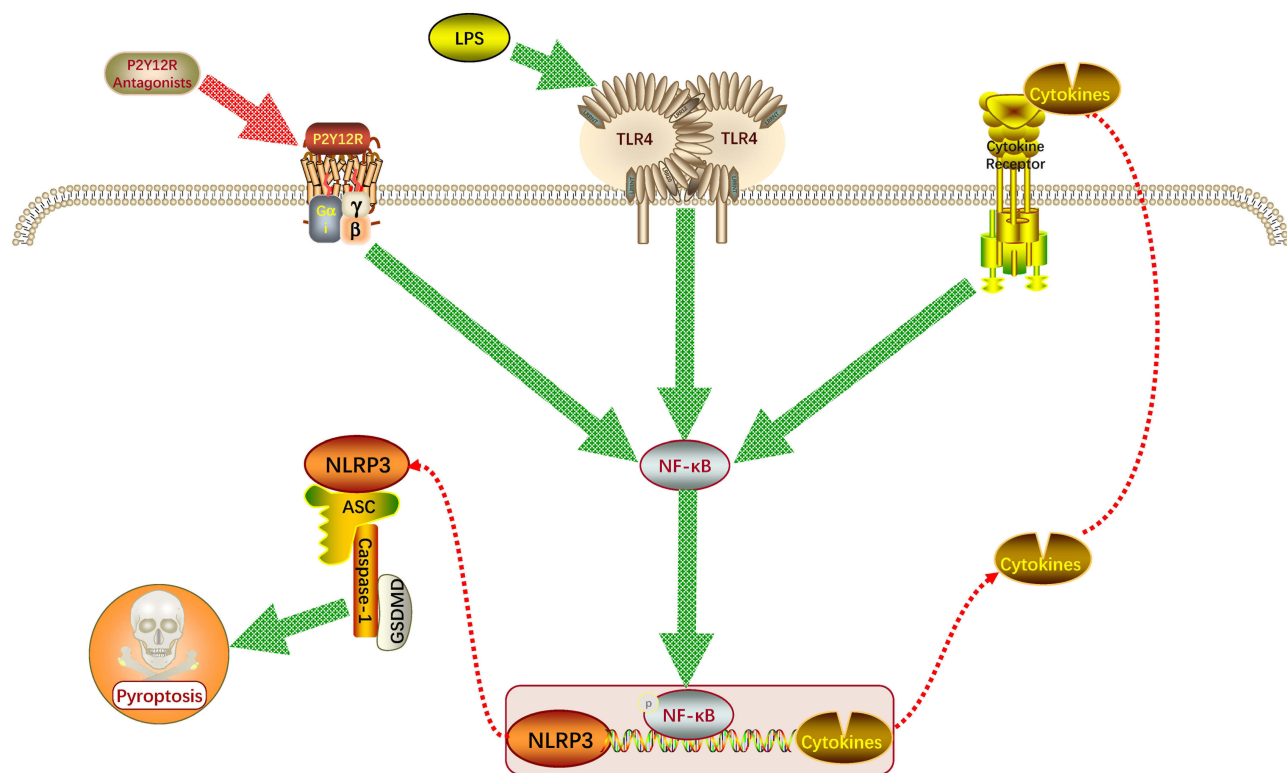


Figure 10 Proposed mechanism of P2Y12 receptor (P2Y12R) antagonists in attenuating lipopolysaccharide (LPS)-induced inflammation and pyroptosis. LPS activates TLR4, leading to the downstream activation of NF- κ B, which subsequently promotes the expression of pro-inflammatory cytokines and inflammasome components, including NLRP3, ASC, Caspase-1, and GSDMD. This results in pyroptosis, a form of programmed cell death contributing to tissue injury. P2Y12R antagonists (Ticagrelor, Prasugrel, Clopidogrel) inhibit P2Y12R signaling, reducing NF- κ B activation and inflammasome assembly. The green arrows represent the inhibitory effects of P2Y12R antagonists on key inflammatory pathways, while the red dashed lines indicate the pyroptotic cascade mediated by inflammasome activation and cytokine release. The red dashed lines indicate the caspase-1-mediated maturation and release of the pyroptotic cytokines IL-1 β and IL-18 via GSDMD pores, both of which were significantly reduced by P2Y12R antagonist treatment in this study.

Our histological and biochemical analyses revealed that LPS exposure triggered extensive lung tissue damage, as evidenced by alveolar wall thickening, inflammatory cell infiltration, increased protein leakage into the BALF, and elevated lung wet/dry weight ratio. These pathological changes are consistent with previous studies using LPS to induce ALI and replicate key clinical features of the condition.^{21,22} Treatment with P2Y12R antagonists, particularly Ticagrelor, significantly attenuated these structural and functional abnormalities, indicating that P2Y12R signaling inhibition contributes to the attenuation of LPS-ALI progression.

LPS-induced inflammation is a well-established model of ALI, where LPS activates the innate immune system via TLR4, leading to downstream activation of NF- κ B and the production of pro-inflammatory cytokines.²³ These cytokines play an important role in the initiation and amplification of the inflammatory response, creating a self-perpetuating cycle of inflammation that ultimately results in alveolar-capillary barrier disruption and impaired gas exchange.^{24,25} A central finding of our study is the substantial reduction of inflammatory cytokines and chemokines following P2Y12R antagonist treatment. LPS challenge robustly increased the levels of IL-1 β , IL-6, TNF- α , IL-12, IL-23, CXCL-1, MCP-1, and G-CSF, which are critical mediators of neutrophil recruitment, cytokine amplification, and tissue injury in ALI. Conversely, the anti-inflammatory cytokine IL-10 was suppressed by LPS but restored following P2Y12R blockade. These changes indicate that P2Y12R signaling plays a role in regulating the cytokine milieu during ALI. Notably, the superior efficacy of Ticagrelor in reducing cytokine levels may be attributed to its dual mechanism of action. Besides P2Y12R antagonism, it also inhibits adenosine reuptake, thereby increasing extracellular adenosine concentrations and enhancing anti-inflammatory signaling via A2A receptors.

NF- κ B is a critical transcription factor that regulates the expression of pro-inflammatory genes in response to various stimuli, including LPS.^{26,27} It has been extensively implicated in the pathogenesis of ALI, where its activation leads to

the expression of numerous inflammatory mediators that contribute to tissue damage. Immunofluorescence analysis revealed that LPS stimulation induced marked phosphorylation of NF- κ B in lung tissue, which was significantly attenuated by all three P2Y₁₂R antagonists. These results suggest that P2Y₁₂R blockade disrupts upstream signaling events necessary for NF- κ B activation, thereby limiting the inflammatory cascade, which was consistent with the previous studies showing that Clopidogrel, Prasugrel, and Ticagrelor could inhibit NF- κ B activation during inflammation.^{28–30} While we did not observe significant changes in TLR4 or P2Y₁₂R protein levels in lung tissue, the functional inhibition of P2Y₁₂R appears sufficient to reduce downstream NF- κ B activation.

Pyroptosis, a form of programmed cell death driven by the activation of the NLRP3 inflammasome, has recently gained attention for its role in inflammation and tissue injury in ALI.³¹ This process is initiated when danger signals activate the NLRP3 inflammasome complex, which in turn cleaves and activates caspase-1.³² Active caspase-1 then processes pro-IL-1 β and pro-IL-18 into their mature forms while simultaneously cleaving GSDMD to form plasma membrane pores.³³ The resulting cell lysis releases inflammatory contents into the extracellular space, further amplifying the local inflammatory response.³⁴ A major innovation of our study lies in the exploration of pyroptosis as a downstream consequence of P2Y₁₂R signaling in ALI. Our data showed that LPS significantly upregulated NLRP3, ASC, Caspase-1, GSDMD levels, as well as the mature IL-1 β and IL-18 levels in lung tissue, consistent with active inflammasome assembly and pyroptotic signaling. Importantly, treatment with P2Y₁₂R antagonists markedly suppressed the expression of these inflammasome components, indicating that P2Y₁₂R activity promotes pyroptosis during ALI. By inhibiting this process, P2Y₁₂R antagonists not only limit cytokine production but also reduce cell death and structural damage. In parallel to our present study, previous study found that pre-treatment with ticagrelor suppressed myocardial ischemia-reperfusion injury-induced upregulation of NLRP3, ASC, and caspase-1, and thus inhibiting pyroptosis in lung.³⁵ Clopidogrel was also shown to decrease brain pyroptosis by inactivating NF- κ B/NLRP3/caspase-1/GSDMD signaling pathway.²⁸ In addition to reductions in NLRP3/caspase-1/GSDMD levels, our flow cytometry data directly confirmed inhibition of pyroptotic cell death. The decrease in Annexin V+/PI+ cells after treatment with P2Y₁₂R antagonists provides functional validation that suppression of the inflammasome axis translates into reduced pyroptosis at the cellular level.

The ultrastructural integrity of lung tissue was assessed using TEM, providing additional evidence of cellular injury and its attenuation by P2Y₁₂R blockade.³⁶ LPS exposure led to prominent mitochondrial swelling, endoplasmic reticulum dilation, and vacuole formation, hallmark features of cellular stress and death.³⁷ In contrast, lung tissues from Ticagrelor-, Prasugrel-, and Clopidogrel-treated mice exhibited reduced organelle damage and preserved cell architecture. These findings corroborate our molecular data and suggest that inhibition of pyroptosis by P2Y₁₂R antagonists translates into tangible cellular protection.

Among the three agents tested, Ticagrelor consistently demonstrated superior efficacy in improving histological outcomes, suppressing pro-inflammatory cytokines, and inhibiting pyroptosis. This may be partly due to its unique pharmacological properties. Unlike Clopidogrel and Prasugrel, which require hepatic activation and irreversibly bind P2Y₁₂R,³⁸ Ticagrelor is a reversible, direct-acting antagonist that also increases extracellular adenosine levels.^{39,40} Adenosine, acting via A_{2A} and A_{2B} receptors, exerts potent anti-inflammatory and tissue-protective effects, including suppression of neutrophil infiltration, inhibition of NF- κ B signaling, and promotion of epithelial repair.^{41,42} Therefore, the dual actions of Ticagrelor may explain its enhanced performance in our ALI model.

P2Y₁₂R is best known for its expression on platelets but is also found on various immune cells, including macrophages, dendritic cells, and subsets of T lymphocytes. In the lung, alveolar macrophages are likely a key target, as they are central to NLRP3 inflammasome activation and IL-1 β /IL-18 release. However, other cell types such as neutrophils, epithelial cells, and endothelial cells may also contribute to the observed responses. Our analyses were performed in whole lung tissue and BALF, which capture the integrated inflammatory milieu but do not distinguish cell-specific effects. Future studies using flow cytometry with intracellular staining, immunofluorescence colocalization, or conditional knockout models will be required to determine whether the protective effects of P2Y₁₂R antagonists are primarily mediated through alveolar macrophages or extend to other cell populations in ALI. On the other hand, pyroptosis can be mediated not only by the canonical NLRP3/caspase-1 pathway but also by the non-canonical caspase-11 pathway, which senses intracellular LPS and cleaves GSDMD independently of caspase-1. Our study focused on the canonical pathway and confirmed inhibition of NLRP3, ASC, caspase-1 activation, and GSDMD cleavage by P2Y₁₂R antagonists. We did not measure caspase-11 expression or activation, which

represents a limitation. Further studies are warranted to assess whether P2Y₁₂R antagonists also influence the caspase-11 pathway in LPS-induced ALI, which would provide additional mechanistic support.

Although our study provides compelling evidence for the anti-inflammatory and anti-pyroptotic effects of P2Y₁₂R antagonists, several limitations should be acknowledged. First, we used a single model of ALI induced by LPS, which may not capture the complexity of other etiologies such as trauma, sepsis, or viral infections. Second, although we demonstrated changes in key signaling proteins, mechanistic validation using genetic models or inflammasome-specific inhibitors would strengthen the causal links. Thirdly, future studies should evaluate whether delayed administration of P2Y₁₂R antagonists after LPS challenge retains therapeutic efficacy, which would have more clinical relevance. Lastly, although the markers used in the present study are canonical for inflammasome-mediated pyroptosis, they do not absolutely exclude contributions from other programmed death pathways such as apoptosis, necroptosis, or ferroptosis in the complex inflammatory lung environment. Additionally, we did not employ genetic models (such as NLRP3-, caspase-1-, or GSDMD-knockout mice) or pharmacologic inhibitors, which would provide direct causal validation. On the other hand, our flow cytometry readout (Annexin V+/PI+) is widely used to detect membrane rupture but may overlap with late necrotic populations. Future studies using genetic approaches and pathway-specific inhibitors will be important to definitively confirm the indispensability of inflammasome-driven pyroptosis in ALI and to clarify the contribution of parallel cell death pathways.

Conclusion

In conclusion, our study demonstrated that P2Y₁₂R antagonists, especially Ticagrelor, protected against LPS-induced ALI by suppressing NF- κ B-mediated inflammation and inhibiting NLRP3-dependent pyroptosis. These findings indicated P2Y₁₂R could be served as a promising target for therapeutic intervention in inflammatory lung diseases and suggested that antiplatelet agents could be repurposed to modulate innate immunity and improve pulmonary outcomes. Further clinical and translational studies are warranted to validate these observations and explore the therapeutic potential of P2Y₁₂R blockade in ALI and ARDS.

Acknowledgments

This work was supported by Fujian Provincial Natural Science Foundation of China [2023J011691] and Natural Science Foundation of Xiamen, China [3502Z202373087]. We would like to thank Instrumental Analysis Center of Huaqiao University for the help of confocal testing.

Disclosure

The authors declare that there is no conflict of interest.

References

1. Wheeler AP, Bernard GR. Acute lung injury and the acute respiratory distress syndrome: a clinical review. *Lancet*. 2007;369(9572):1553–1564. doi:10.1016/S0140-6736(07)60604-7
2. Toy P, Looney MR, Popovsky M, et al. Transfusion-related acute lung injury: 36 years of progress (1985–2021). *Ann Am Thorac Soc*. 2022;19(5):705–712. doi:10.1513/AnnalsATS.202108-963CME
3. Hoshino T, Yoshida T. Future directions of lung-protective ventilation strategies in acute respiratory distress syndrome. *Acute Med Surg*. 2024;11(1):e918. doi:10.1002/ams2.918
4. Lian J, Lin J, Zakaria N, Yahaya BH. Acute lung injury: disease modelling and the therapeutic potential of stem cells. *Adv Exp Med Biol*. 2020;1298:149–166. doi:10.1007/5584_2020_538
5. Xiao J, Wang L, Zhang B, Hou A. Cell death in acute lung injury: caspase-regulated apoptosis, pyroptosis, necroptosis, and PANoptosis. *Front Pharmacol*. 2025;16:1559659. doi:10.3389/fphar.2025.1559659
6. Wang J, Li LL, Zhao ZA, Niu CY, Zhao ZG. NLRP3 Inflammasome-mediated pyroptosis in acute lung injury: roles of main lung cell types and therapeutic perspectives. *Int Immunopharmacol*. 2025;154:114560. doi:10.1016/j.intimp.2025.114560
7. Wang C, Liu N. Bibliometric analysis of pyroptosis in pathogenesis and treatment of acute lung injury. *Front Med*. 2024;11:1488796. doi:10.3389/fmed.2024.1488796
8. Luo L, Zhuang X, Fu L, et al. The role of the interplay between macrophage glycolytic reprogramming and NLRP3 inflammasome activation in acute lung injury/acute respiratory distress syndrome. *Clin Transl Med*. 2024;14(12):e70098. doi:10.1002/ctm2.70098
9. Cattaneo M. P2Y₁₂ receptors: structure and function. *J Thromb Haemost*. 2015;13(Suppl 1):S10–6. doi:10.1111/jth.12952
10. Chen XY, Wang K, Jia J, Kong XT, Li HQ, Tian S. P2Y₁₂R antagonists in antithrombotic therapy: a patent and literature review (2019-present). *Expert Opin Ther Pat*. 2025;35(5):515–532. doi:10.1080/13543776.2025.2467683

11. Andersen LL, Huang Y, Urban C, et al. Systematic P2Y receptor survey identifies P2Y11 as modulator of immune responses and virus replication in macrophages. *EMBO J.* 2023;42(23):e113279. doi:10.15252/embj.2022113279
12. Le Duc D, Schulz A, Lede V, et al. P2Y receptors in immune response and inflammation. *Adv Immunol.* 2017;136:85–121. doi:10.1016/bs.ai.2017.05.006
13. Wu XM, Zhang N, Li JS, Yang ZH, Huang XL, Yang XF. Purinergic receptors mediate endothelial dysfunction and participate in atherosclerosis. *Purinergic Sig.* 2023;19(1):265–272. doi:10.1007/s11302-021-09839-x
14. Chen Y, Wang C, Wu Y, et al. Magnesium isoglycyrrhizinate alleviates alectinib-induced hepatotoxicity by inhibiting mitochondrial damage-mediated pyroptosis. *Drug Des Devel Ther.* 2025;19:6219–6233. doi:10.2147/DDDT.S523455
15. Luo D, Ji HJ, Yan XQ, et al. Run-Mu-Ling granules mitigate ocular surface inflammatory injury associated with dry eye by suppressing the NLRP3/GSDMD-mediated pyroptosis pathway. *J Inflamm Res.* 2024;17:10769–10784. doi:10.2147/JIR.S496231
16. Lee EJ, Lee SM, Oh JH, et al. Ticagrelor, but not clopidogrel, attenuates hepatic steatosis in a model of metabolic dysfunction-associated steatotic liver disease. *Nutrients.* 2024;16(7):920. doi:10.3390/nu16070920
17. Ogawa T, Hashimoto M, Niitsu Y, et al. Effects of prasugrel, a novel P2Y(12) inhibitor, in rat models of cerebral and peripheral artery occlusive diseases. *Eur J Pharmacol.* 2009;612(1–3):29–34. doi:10.1016/j.ejphar.2009.03.073
18. Yoshikawa N, Xia M, Nakamura K. Inhibitory effect of clopidogrel, a P2Y(12) receptor antagonist, on hematogenic metastasis in B16-BL6 mouse melanoma cells. *In Vivo.* 2025;39(3):1325–1330. doi:10.21873/invivo.13936
19. Qiu Y, Gao J, Chu W, et al. ZIF-8 as efficient carriers for polysaccharide from *Tetrastigma Hemsleyanum* Diels et Gilg in acute lung injury induced by lipopolysaccharides. *Int J Biol Macromol.* 2024;283(Pt 4):137966. doi:10.1016/j.ijbiomac.2024.137966
20. Kim SY, Yoon JH, Jung DH, Kim GH, Kim CH, Lee SK. Fexuprazan safeguards the esophagus from hydrochloric acid-induced damage by suppressing NLRP1/Caspase-1/GSDMD pyroptotic pathway. *Front Immunol.* 2024;15:1410904. doi:10.3389/fimmu.2024.1410904
21. Jiang Z, He R, Zhong Y, Liu B, He Z. Fumarate hydratase restrains mtDNA attenuates LPS-induced acute lung injury through cGAS-STING pathways. *J Inflamm Res.* 2025;18:5399–5413. doi:10.2147/JIR.S518589
22. Qian M, Zhu Y, Lin W, et al. PICK1 overexpression ameliorates endotoxin-induced acute lung injury by regulating mitochondrial quality control via maintaining Nrf-2 stabilization through activating the PI3K/Akt/GSK-3beta pathway and disrupting the E3 ubiquitin ligase adapter beta-TrCP. *Int Immunopharmacol.* 2025;156:114685. doi:10.1016/j.intimp.2025.114685
23. Al-Naimi MS, Abu-Raghib AR, Mansoor AFA, Fawzi HA. Isofraxidin attenuates lipopolysaccharide-induced cytokine release in mice lung and liver tissues via inhibiting inflammation and oxidative stress. *Biomedicines.* 2025;13(3):653. doi:10.3390/biomedicines13030653
24. Liu C, Chu D, Kalantar-Zadeh K, George J, Young HA, Liu G. Cytokines: from clinical significance to quantification. *Adv Sci.* 2021;8(15):e2004433. doi:10.1002/advs.202004433
25. Yu H, Lin L, Zhang Z, Zhang H, Hu H. Targeting NF-kappaB pathway for the therapy of diseases: mechanism and clinical study. *Signal Transduct Target Ther.* 2020;5(1):209. doi:10.1038/s41392-020-00312-6
26. Watabe Y, Giam chuang VT, Sakai H, et al. Carbon monoxide alleviates endotoxin-induced acute lung injury via NADPH oxidase inhibition in macrophages and neutrophils. *Biochem Pharmacol.* 2025;233:116782. doi:10.1016/j.bcp.2025.116782
27. Wang Y, Li B, Zhang Y, Lu R, Wang Q, Gao Y. Qingfei Huoxue decoction and its active component narirutin alleviate LPS-induced acute lung injury by regulating TLR4/NF-kappaB pathway mediated inflammation. *J Inflamm Res.* 2024;17:7503–7520. doi:10.2147/JIR.S480101
28. Li F, Xu D, Hou K, et al. Pretreatment of Indobufen and Aspirin and their combinations with clopidogrel or ticagrelor alleviates inflammasome mediated pyroptosis via inhibiting NF-kappaB/NLRP3 pathway in ischemic stroke. *J Neuroimmune Pharmacol.* 2021;16(4):835–853. doi:10.1007/s11481-020-09978-9
29. Satonaka H, Nagata D, Takahashi M, et al. Involvement of P2Y12 receptor in vascular smooth muscle inflammatory changes via MCP-1 upregulation and monocyte adhesion. *Am J Physiol Heart Circ Physiol.* 2015;308(8):H853–61. doi:10.1152/ajpheart.00862.2013
30. Jia Z, Huang Y, Ji X, Sun J, Fu G. Ticagrelor and clopidogrel suppress NF-kappaB signaling pathway to alleviate LPS-induced dysfunction in vein endothelial cells. *BMC Cardiovasc Disord.* 2019;19(1):318. doi:10.1186/s12872-019-01287-1
31. Zheng Q, Mei G, Cheng P, Li Y, Zhang Q, Ye M. Exploration of omega-9MUFAs: mitigating effect on lipopolysaccharide-induced acute lung injury. *Eur J Pharmacol.* 2025;998:177396. doi:10.1016/j.ejphar.2025.177396
32. Swanson KV, Deng M, Ting JP. The NLRP3 inflammasome: molecular activation and regulation to therapeutics. *Nat Rev Immunol.* 2019;19(8):477–489. doi:10.1038/s41577-019-0165-0
33. Van Opendenbosch N, Lamkanfi M. Caspases in cell death, inflammation, and disease. *Immunity.* 2019;50(6):1352–1364. doi:10.1016/j.immuni.2019.05.020
34. Chai R, Li Y, Shui L, Ni L, Zhang A. The role of pyroptosis in inflammatory diseases. *Front Cell Dev Biol.* 2023;11:1173235. doi:10.3389/fcell.2023.1173235
35. Dai YN, Wang LT, Zhang YS, et al. Ticagrelor alleviates pyroptosis of myocardial ischemia reperfusion-induced acute lung injury in rats: a preliminary study. *PeerJ.* 2024;12:e16613. doi:10.7717/peerj.16613
36. Lang D, Stoiber W, Lohfink-Schumm S, et al. Transmission electron microscopy of transbronchial lung cryobiopsy samples in a cohort of fibrotic interstitial lung disease patients - feasibility and implications of endothelial alterations. *Respir Res.* 2024;25(1):366. doi:10.1186/s12931-024-02981-1
37. Esteves AR, Silva DF, Banha D, Candeias E, Guedes B, Cardoso SM. LPS-induced mitochondrial dysfunction regulates innate immunity activation and alpha-synuclein oligomerization in Parkinson's disease. *Redox Biol.* 2023;63:102714. doi:10.1016/j.redox.2023.102714
38. Teng R. Ticagrelor: pharmacokinetic, pharmacodynamic and pharmacogenetic profile: an update. *Clin Pharmacokinet.* 2015;54(11):1125–1138. doi:10.1007/s40262-015-0290-2
39. Goel D. Ticagrelor: the first approved reversible oral antiplatelet agent. *Int J Appl Basic Med Res.* 2013;3(1):19–21. doi:10.4103/2229-516X.112234
40. Khalil J, Dimofte T, Roberts T, et al. Ticagrelor inverse agonist activity at the P2Y(12) receptor is non-reversible versus its endogenous agonist adenosine 5'-diphosphate. *Br J Pharmacol.* 2024;181(1):21–35. doi:10.1111/bph.16204
41. Csoka B, Selmeczy Z, Koscsó B, et al. Adenosine promotes alternative macrophage activation via A2A and A2B receptors. *FASEB J.* 2012;26(1):376–386. doi:10.1096/fj.11-190934
42. Shaikh G, Cronstein B. Signaling pathways involving adenosine A2A and A2B receptors in wound healing and fibrosis. *Purinergic Sig.* 2016;12(2):191–197. doi:10.1007/s11302-016-9498-3

Drug Design, Development and Therapy

Dovepress
Taylor & Francis Group

Publish your work in this journal

Drug Design, Development and Therapy is an international, peer-reviewed open-access journal that spans the spectrum of drug design and development through to clinical applications. Clinical outcomes, patient safety, and programs for the development and effective, safe, and sustained use of medicines are a feature of the journal, which has also been accepted for indexing on PubMed Central. The manuscript management system is completely online and includes a very quick and fair peer-review system, which is all easy to use. Visit <http://www.dovepress.com/testimonials.php> to read real quotes from published authors.

Submit your manuscript here: <https://www.dovepress.com/drug-design-development-and-therapy-journal>